PHYSICAL REVIEW B **73**, 201402(R) (2006)

Charge sensing in carbon-nanotube quantum dots on microsecond timescales

M. J. Biercuk,[1] D. J. Reilly,[1,2] T. M. Buehler,[2] V. C. Chan,[2] J. M. Chow,[1] R. G. Clark,[2] and C. M. Marcus[1]
[1]*Department of Physics, Harvard University Cambridge, Massachusetts 02138, USA*
[2]*Centre for Quantum Computer Technology, School of Physics, University of New South Wales, Sydney 2052, Australia*
(Received 4 January 2006; published 19 May 2006)

We report fast, simultaneous charge sensing and transport measurements of gate-defined carbon nanotube quantum dots. Aluminum radio-frequency (rf) single electron transistors capacitively coupled to the nanotube dot provide single-electron charge sensing on microsecond timescales. Simultaneously, rf reflectometry allows the fast measurement of transport through the nanotube dot. Charge stability diagrams for the nanotube dot in the Coulomb blockade regime show extended Coulomb diamonds into the high-bias regime, as well as even-odd filling effects, revealed in charge sensing data.

DOI: 10.1103/PhysRevB.73.201402 PACS number(s): 73.21.La, 73.22.Dj, 73.23.Hk

Carbon nanotubes are promising systems on which to base coherent electronic devices.[1–3] Due to a combination of strong confinement, quantized phonon spectrum,[4] and zero nuclear spin, carbon nanotubes are likely to exhibit long-lived coherent states. Key to the success of this technology is the ability to manipulate electron states within a nanotube and to perform fast, efficient readout. Recent advances in device fabrication[3,5–8] allow the creation of multiple quantum dots along the length of a tube with controllable coupling by applying voltage biases to electrostatic top gates. However, readout of these structures has been limited to dc transport, which is invasive and slow compared to relevant coherence times.[9]

In this Rapid Communication, we describe the integration of superconducting aluminum radio-frequency single-electron transistors (rf-SETs)[10] with carbon nanotube quantum dot devices defined by electrostatic gates.[8] The rf-SET serves as a sensitive electrometer[11] and, when capacitively coupled to the nanotube dot, provides a means of noninvasively detecting its charge state on short timescales and in regimes not accessible with transport measurements.[12–16] These represent the first charge sensing experiments with nanotube quantum dots using integrated charge detection. In addition, we make use of radio-frequency (rf) reflectometry[17] that enables fast transport measurements of the nanotube correlated with fast charge sensing by the capacitively coupled rf-SET. Previous work[17,18] has used reflectometry to investigate the microwave impedance and charge sensitivity of nanotubes. The present study advances previous works by simultaneously carrying out charge sensing together with rf transport as well as by gaining 5 orders of magnitude in time-domain resolution.

Carbon nanotubes were grown from patterned Fe catalyst islands on a Si/SiO_2 wafer via chemical vapor deposition. Single-walled tubes with diameters less than ~4 nm were identified using atomic force microscopy and selectively contacted via electron beam lithography.[3] Contacts made from ~15 nm of Pd[6] were connected to larger metallic pads defined by optical lithography. The entire device was then coated with ~35 nm Al_2O_3 using low-temperature atomic layer deposition (ALD). Three top gates were then aligned to each nanotube: two "barrier gates" (B1, B2) to deplete the underlying nanotube, defining a quantum dot, with a third "plunger gate" (P) between them to tune the energy of the dot [Fig. 1(a)].[8] The doped Si wafer also serves as a global backgate. Nanotubes that showed little gate response (presumably metallic) were not studied further. The SET island and the nanotube dot were capacitively coupled by a 50 nm Ti/AuPd (20 Å/30 Å) antenna that crosses the tube and sits under the SET island. The aluminum SET was fabricated using double-angle evaporation on top of the coupling antenna [Fig. 1(a)]. Devices were mounted on a circuit board with rf coplanar waveguides and cooled in a dilution refrigerator with a base temperature of 30–50 mK. Electron temperature measured in a similar configuration was in the range of 100–200 mK. Data from two integrated rf-SET-nanotube devices showing similar behavior are reported.

Charge sensing is performed by monitoring the resistance of the SET using rf reflectometry. In the same way, direct transport measurements of the nanotube are made using a small (μV) ac signal at rf frequencies (above 100 MHz). A schematic of the setup, showing the generation of the reflectometry "carrier" signals at frequencies f_1 and f_2, is shown in Fig. 1(b). The two carrier signals are combined onto a single transmission line and fed to a directional coupler at the 1 K stage of the dilution refrigerator. Two tank circuits transform the high resistance of the SET (~50 kΩ) or nanotube (~200 kΩ) toward ~50 Ω, at the resonance frequencies $f_{1,2}$ set by the parasitic capacitance C_p and series chip inductor (L=780 nH for the nanotube and L=330 nH for the SET). At resonance, changes in resistance of either the nanotube or the SET modify the Q factor of the respective tank circuit and the amount of reflected rf power. After amplification at 4 K (40 dB) and room temperature (45 dB) the signals are homodyne detected using two mixers and two local oscillators. Low-pass filtered output voltages from each mixer are proportional to the change in respective device resistance. The use of frequency-domain multiplexing allows both the SET and the nanotube to be monitored using a common transmission line and cryogenic amplifier.[19,20] Bias tees on the circuit board enable standard dc transport measurements of both devices.

Figure 1(c) shows reflected power $S11$ from the tank circuits as a function of frequency measured with a network analyzer after amplification. The two resonances are identified at $f_1 \sim 120$ MHz for the nanotube and $f_2 \sim 165$ MHz for the SET. Bandwidths are ~1 MHz for the nanotube and ~10 MHz for the SET.

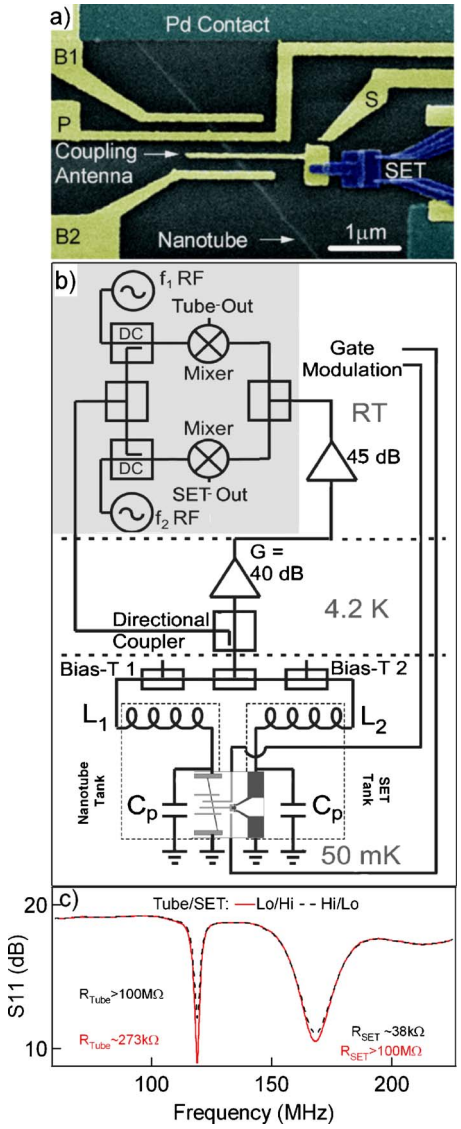

FIG. 1. (a) (Color online) False-color SEM image of a representative nanotube quantum dot device with integrated rf-SET. The nanotube is visible under Al_2O_3 and the Pd contact (top). Gates (yellow or light gray) are labeled on the figure. The rf-SET (blue or dark gray) is aligned to a coupling antenna running over the nanotube. (b) Schematic of the measurement setup for the multiplexed rf reflectometry. The shaded area is the demodulation circuit. (c) Reflected rf signal as measured with a network analyzer for different values of nanotube and SET resistances. In this trace, the nanotube resistance is controlled with the backgate, while that of the SET is changed by shifting the bias voltage in or out of the superconducting gap.

Figure 2(a) shows a charge stability plot for the SET used for all measurements in Figs. 2 and 3. Plotted is the demodulated voltage as a function of both the dc source-drain bias V_{SD}^{SET} across the SET and the voltage applied to a nearby gate. The SET is typically operated at the threshold for quasiparticle transport, $V_{SD}^{SET} \sim 4\Delta/e$ (Δ is the superconducting gap), where the rf-SET sensitivity is maximized. Similar rf-SET devices measured in this setup exhibited charge sensitivities better than $\delta q = 10^{-5} e/\sqrt{\text{Hz}}$.[20]

We form a quantum dot in the carbon nanotube by applying appropriate voltages to gates B1 and B2 [Fig. 1(a)] with the backgate set such that the nanotube is *n*—type. The section of the nanotube between depletion regions formed by gates B1 and B2 serves as the quantum dot. In this configuration, Coulomb blockade (CB) is observed using standard low-frequency lock-in measurements, as a series of conductance peaks as a function of P-gate voltage[8] [Fig. 2(b)].

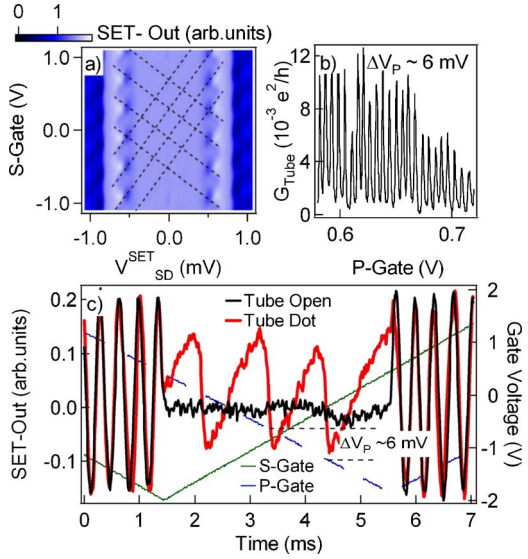

FIG. 2. (Color online) (a) Charge stability diamonds for a superconducting rf-SET. Plotted on the intensity axis is the demodulated signal SET-Out. Dark blue (dark gray) corresponds to ~50 kΩ and light blue (light gray) ~100 MΩ. Dashed lines indicate conditions for resonant Cooper-pair tunneling. (b) Coulomb blockade in the nanotube as measured using standard lock-in techniques with gates B1 and B2 near 2 V, backgate=18 V, V_{SD} =1.5 mV. ΔV_P is the CB peak spacing in gate voltage. Due to a lithography error, gate B2 re-crosses the tube near the drain electrode in this device. (c) SET-Out signal (averaged 60 times, left axis) in the time domain (arbitrary offset) with the SET biased to a sensitive region. Green (continuous gray) and blue (dashed dark gray) traces are the applied triangle wave gate ramps for S- and P-gates (before −40 dB of attenuation), respectively, (right axis). When no dot is formed in the nanotube (B1=B2=10 V), we observe a flat line in the compensated rf-SET response, while forming a dot as in panel (b) yields a sawtooth charge sensing signal.

The energy of the dot is changed on fast timescales by applying a triangle-wave voltage ramp to the P-gate. A compensating gate ramp is applied to the S-gate to maintain the SET at a fixed conductance value. When the P- and S-gates sweep together in the same direction, the SET is uncompensated and exhibits Coulomb blockade. In the region where the P- and S-gates sweep in opposite directions, the SET is compensated and may be held at a position of maximum transconductance.

In the compensated configuration, the SET senses a characteristic sawtooth charging pattern associated with P-gate-induced tunneling of electrons onto the dot. The period of the sawtooth in P-gate voltage is consistent with that measured directly from low-frequency lock-in measurements of CB in the nanotube. By contrast, if the barrier gate voltages are set such that there is no dot formed in the tube, we observe a smooth line in the SET response [black trace, Fig. 2(c)]. This

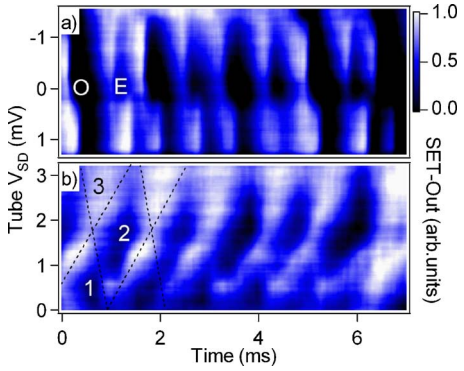

FIG. 3. (Color online) (a) SET signal as a function of time (with a P-gate ramp applied) and V_{SD} across the nanotube showing even (E) and odd (O) filling of energy states in the nanotube quantum dot. (b) Similar measurements in a different configuration of B1 and B2 showing first-, second-, and third-order Coulomb diamonds with increasing V_{SD}. Dashed lines are guides to the eye indicating the boundaries of diamonds in which the charge number on the dot is fixed.

indicates that the observed sawtooth response corresponds to the charging of the gate-defined nanotube quantum dot. The magnitude of the charge signal induced on the SET with the addition of a single electron to the nanotube dot is $\sim 0.2e$, indicating strong coupling between the nanotube and the SET electrometer.

Plotting the (compensated) SET-Out signal as a function of time (as the P-gate voltage is ramped) and source-drain voltage V_{SD} across the tube reveals the familiar diamond pattern associated with Coulomb blockade [Fig. 3(a)]. Here, the applied voltage V_{SD} across the nanotube also couples capacitively to the SET itself. This effect is nulled by adding a compensating dc offset to the gate ramp. The nanotube dot charge configuration is fixed in the diamond regions (and current blocked), while the blockade is lifted and current flow allowed at sufficiently high values of V_{SD}. In appropriate biasing configurations of gates B1 and B2, we observe even-odd filling in the nanotube quantum dot,[21] indicated by an alternating pattern of large and small diamonds. This is consistent with a shell-filling model in which a single electron can enter a discrete energy level in the dot with charging energy $E_c = e^2/2C$ and quantum level spacing ΔE (C is the total dot capacitance). A second electron, with opposite spin to the first can enter the same orbital state requiring only E_c. Estimating ΔE for a dot of the size used in this experiment to be $\Delta E = 750\ \mu$V using $E = h v_F/2L$, where $L \sim 1\ \mu$m is the dot length, is consistent with experimental measurements. We have also observed fourfold shell filling[22,23] in these gated nanotube devices.

In addition to the low-bias diamonds commonly visible in transport, charge sensing enables detection of the Coulomb staircase in V_{SD} when one of the tunnel barriers is made much larger than the other. In this configuration, consecutive Coulomb levels are populated from the source with increasing V_{SD} before tunneling to the drain can occur. Detection is possible because the SET senses the charge state of the nanotube dot and not the current that flows from source to drain, which can be immeasurably small when the resistance of one

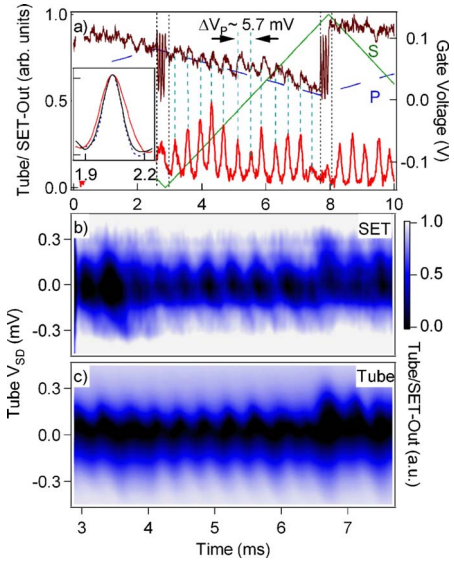

FIG. 4. (Color online) (a) Fast, simultaneous measurement of the rf-SET and nanotube using rf reflectometry at tube $V_{SD} \sim 250\ \mu$V. CB peaks are evident in the nanotube signal (lower trace) corresponding to a sawtooth in SET-Out (upper trace). CB is also evident in the SET signal at points where the gate biases change sweep direction and the SET is uncompensated (within the dotted lines). B1, B2 ~ 0 V, backgate=7.78 V. Inset: (lower left corner) shows the backaction dependence of a CB peak in the tube as measured using reflectometry at different V_{SD}^{SET}: biased to the gap (black solid trace), biased to the double Josephson quasiparticle peak (dashed trace) and $\sim$V (red or light gray solid trace). (b) and (c) A logarithmic intensity plot of SET-Out and Tube-Out, respectively, [gate ramps identical to those in panel (a)] as a function of V_{SD} across the tube. Coulomb diamonds are visible in both panels, with key features reproduced between both. Each sweep at fixed V_{SD} has been averaged 1000 times.

of the barriers is made large enough to observe the Coulomb staircase. In the SET sensing signal, we observe diamonds centered at $V_{SD} = e/2C$, the bias corresponding to the apex of the first-order charging diamonds. First-, second-, and the beginning of third-order diamonds are visible in Fig. 3(b), each offset by $e/2C$ from the center of the diamonds of the next lower or higher order.[24]

By monitoring the demodulated signals from the tube and SET simultaneously, we can correlate rf transport and charge sensing. Figure 4(a) shows both the demodulated signal from the nanotube together with SET-Out for S- and P-gate ramps with the nanotube in the CB regime (different device from Figs. 2 and 3). CB peaks are evident in the signal from the tube, and a sawtooth pattern is visible in SET-Out, with sequential charge addition occurring on timescales of $\sim 300\ \mu$s (we have performed similar measurements with charge addition periods $\sim 30\ \mu$s, but systematic noise increased with gate speed). The two signals are correlated as expected, with the apex of each CB peak falling roughly in the middle of the charging sawtooth. Further, the width of the sharp transition region for each sawtooth is roughly equivalent in time to the width of the CB peak.

We have also studied how the V_{SD}^{SET} biasing point of the SET influences the Coulomb blockade in the nanotube quan-

tum dot. Consistent with measurements made on Al single-electron boxes,[25] we observe asymmetries and changes in the width of the CB peaks with varying V_{SD}^{SET} across the SET [Inset of Fig. 4(a)]. This behavior is likely due to a combination of heating[26] and the backaction connected with charge fluctuations of the SET island as current flows from source to drain. We see a very slight *narrowing* of the Coulomb blockade peaks in the nanotube dot when the rf-SET is biased near the double Josephson quasiparticle peak (DJQP),[27] relative to the CB peak width when the SET is biased into the superconducting gap. Separating backaction and heating effects will require further study.

Charge stability plots for the nanotube quantum dot, constructed from both SET-Out [Fig. 4(b)] and Tube-Out [Fig. 4(c)] as a function of V_{SD} across the nanotube, show the nanotube (peaks) and SET (sawtooth) signals to be correlated. The rf-SET, however, is sensitive to charge fluctuations in regions of V_{SD} and P-gate voltage where direct transport measurements on the tube do not yield measurable currents, and where resistance changes in the nanotube mapped through reflected rf are immeasurable.

In conclusion, we have presented fast rf-reflectometry measurements of a gate-defined quantum dot in a carbon nanotube, in which charge configurations of the nanotube were adjusted and measured on microsecond timescales. With the incorporation of Al rf-SETs we are able to perform noninvasive charge sensing measurements of the quantum dot on fast timescales in correlation with fast reflectometry and standard dc transport measurements of the nanotube itself. Our results demonstrate the feasibility of this technology for fast and near quantum-limited readout of nanotube-based coherent electronic devices. Finally, the use of a nanotube as a fast electrometer and the backaction measurements presented here raise interesting questions about the nature of the (quantum) noise spectrum associated with coherent transport in these devices.

The authors thank D. Barber, R. Starrett, and N. Court for technical assistance. This work was supported by ARO/ARDA (Contract No. DAAD19-02-1-0039, Contract No. DAAD 19-01-1-0191, and Contract No. DAAD19-01-1-0653), NSF-NIRT (Contract No. EIA-0210736), and Harvard Center for Nanoscale Systems. M.J.B. acknowledges support from NSF graduate research and ARO-QCGR. D.J.R. acknowledges support from Hewlett-Packard Corporation.

[1] P. L. McEuen, M. Bockrath, D. H. Cobden, Y.-G. Yoon, and S. G. Louie, Phys. Rev. Lett. **83**, 5098 (1999).

[2] W. Liang, M. Bockrath, D. Bozovic, J. H. Hafner, M. Tinkham, and H. Park, Nature (London) **411**, 665 (2001).

[3] M. J. Biercuk, N. Mason, J. Martin, A. Yacoby, and C. M. Marcus, Phys. Rev. Lett. **94**, 026801 (2005).

[4] J. Hone, B. Batlogg, Z. Benes, A. T. Johnson, and J. E. Fischer, Science **289**, 1730 (2000).

[5] A. Javey, H. Kim, M. Brink, Q. Wang, A. Ural, J. Guo, P. McIntyre, P. McEuen, M. Lundstrom, and H. Dai, Nat. Mater. **1**, 241 (2002).

[6] A. Javey, J. Guo, Q. Wang, M. Lundstrom, and H. Dai, Nature (London) **424**, 654 (2003).

[7] M. J. Biercuk, N. Mason, and C. M. Marcus, Nano Lett. **4**, 2499 (2004).

[8] M. J. Biercuk, S. Garaj, N. Mason, J. M. Chow, and C. M. Marcus, Nano Lett. **5**, 1267 (2005).

[9] L. Forro *et al.*, *Science and Application of Nanotubes* (Kluwer Academic-Plenum, New York, 2000), p. 297).

[10] R. J. Schoelkopf, P. Wahlgren, A. A. Kozhevnikov, P. Delsing, and D. E. Prober, Science **280**, 1238 (1998).

[11] M. H. Devoret and R. J. Schoelkopf, Nature (London) **406**, 1039 (2000).

[12] L. DiCarlo, H. J. Lynch, A. C. Johnson, L. I. Childress, K. Crockett, C. M. Marcus, M. P. Hanson, and A. C. Gossard, Phys. Rev. Lett. **92**, 226801 (2004).

[13] W. Lu, Z. Ji, L. N. Pfeiffer, K. W. West, and A. J. Rimberg, Nature (London) **423**, 422 (2003).

[14] T. M. Buehler, D. J. Reilly, R. P. Starrett, A. D. Greentree, A. R. Hamilton, A. S. Dzurak, and R. G. Clark, Appl. Phys. Lett. **86**, 143117 (2005).

[15] L. M. K. Vandersypen, J. M. Elzerman, R. N. Schouten, L. H. W. van Beveren, R. Hanson, and L. P. Kouwenhoven, Appl. Phys. Lett. **85**, 4394 (2004).

[16] J. M. Elzerman, R. Hanson, L. H. W. van Beveren, B. Witkamp, L. M. K. Vandersypen, and L. P. Kouwenhoven, Nature (London) **430**, 431 (2004).

[17] L. Roschier, M. Sillanpaa, W. Taihong, M. Ahlskog, S. Iijima, and P. Hakonen, J. Low Temp. Phys. **136**, 465 (2004).

[18] S. Li, Z. Yu, S.-F. Yen, W. C. Tang, and P. J. Burke, Nano Lett. **4**, 753 (2004).

[19] T. R. Stevenson, F. A. Pellerano, C. M. Stahle, K. Aidala, and R. J. Schoelkopf, Appl. Phys. Lett. **80**, 3012 (2002).

[20] T. M. Buehler, D. J. Reilly, R. P. Starrett, N. A. Court, A. R. Hamilton, A. S. Dzurak, and R. G. Clark, J. Appl. Phys. **96**, 4508 (2004).

[21] D. H. Cobden, M. Bockrath, P. L. McEuen, A. G. Rinzler, and R. E. Smalley, Phys. Rev. Lett. **81**, 681 (1998).

[22] W. Liang, M. Bockrath, and H. Park, Phys. Rev. Lett. **88**, 126801 (2002).

[23] S. Sapmaz, P. Jarillo-Herrero, J. Kong, C. Dekker, L. P. Kouwenhoven, and H. S. J. van der Zant, Phys. Rev. B **71**, 153402 (2005).

[24] We also observe higher-order diamonds without compensating for the direct effect of V_{SD} on the SET, but over a smaller range of gate bias.

[25] B. A. Turek, K. W. Lehnert, A. Clerk, D. Gunnarsson, K. Bladh, P. Delsing, and R. J. Schoelkopf, Phys. Rev. B **71**, 193304 (2005).

[26] V. A. Krupenin, S. V. Lotkhov, H. Scherer, T. Weimann, A. B. Zorin, F.-J. Ahlers, J. Niemeyer, and H. Wolf, Phys. Rev. B **59**, 10778 (1999).

[27] A. A. Clerk, S. M. Girvin, A. K. Nguyen, and A. D. Stone, Phys. Rev. Lett. **89**, 176804 (2002).